

Molecular Dynamics Study on Liquid-to-Amorphous and Amorphous-to-Crystal Transitions in Ti-Al Alloys

Masato Shimono and Hidehiro Onodera

National Research Institute for Metals, 1-2-1 Sengen, Tsukuba 305, Japan

Liquid-to-amorphous transition and amorphous-to-crystal transition processes of Ti-Al alloys were investigated by using constant-pressure, constant-temperature molecular dynamics techniques. Many-body interactions semi-empirically determined by the Embedded Atom Method were used. Thermodynamic properties obtained in the simulation were in good agreement with experimental measurements. Especially, the present simulation could reproduce the experimentally observed concentration range (40~85 at.% Al) for amorphization. Structure analyses revealed that the basic structure of amorphous states in the Ti-Al system is a network of icosahedral clusters stabilized by many-body effect.

1. INTRODUCTION

With the increasing computational capabilities of modern computer systems, computational materials science has recently become a standard tool in materials research. Among the computational approaches which were proposed, molecular dynamics calculations have made a significant progress in studying both mechanical and thermodynamical material properties from an atomistic point of view.

Ti-Al system is of both technological and theoretical interests because alloys in this system have the excellent high-temperature mechanical properties and because atomic ordering and composition have non-trivial effects on the structural and thermodynamic properties of the alloys. Especially, we have a particular interest on the way of the materials design of these alloys through the microstructural control utilizing the transition process from amorphous state to crystalline state.

Experimental observations¹ indicate that Ti-Al alloys could undergo amorphization in rapid quenching process from gas state such as sputter deposition in somewhat Al-rich concentration range (40~85 at.% Al). At annealing process of thus obtained amorphous state of these alloys, several intermediate metastable states have been observed² during the transition process from amorphous to the most stable crystalline structure. Thus our aim in this work is to understand the microscopic mechanism by which the amorphization or the amorphous-crystal transition takes place in the Ti-Al system by using molecular dynamics techniques.

2. POTENTIALS

We have used many-body interactions derived semi-empirically based on the Embedded Atom Method (EAM)³ in the simulations. The Ti and Al potentials developed by Oh and Johnson⁴ were used after slight modifications. The Ti-Al cross potential was created using Johnson's method⁵. We fit our Ti-Al cross potential to the pair of experimental values⁶ of heats of solution for Ti-Al binary alloys by adjusting one free parameter, which is the relative weight of the Ti and Al electron densities. To focus on many-body effects, 8-4 type Lennard-Jones pair potentials⁷ were also used in another series of simulations.

3. SIMULATION METHODS

Our simulations were performed with the system of 216 atoms in a parallelepipedic cell with periodic boundary conditions along all three directions. The Parrinello-Rahman scheme⁸ was used, in which the simulation cell could vary in size and shape, so that structural transformations should not be restricted by the shape of the cell. The system is kept at a desired temperature by periodic rescaling of the atomic momenta. Numerical integration of the equations of motion is performed by a third-order formalism with a variable time step of order of fs. To calculate the forces we used a spherical cut-off of radius equal to 8 Å.

We have carried out a series of simulations on Ti-Al systems with ten atomic ratios ranging from 0 to 100 at. % Al. In each case, starting from a liquid state at a temperature above the melting point, the system was firstly cooled down to 5 K at various cooling rates

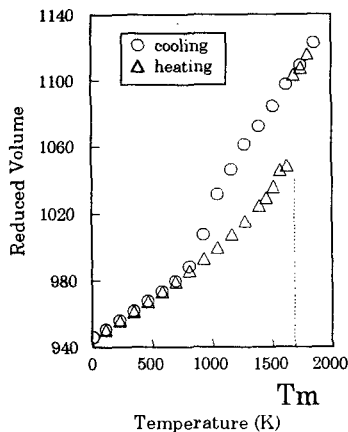


Fig. 1. Temperature dependence of the volume in a cooling and heating cycle.

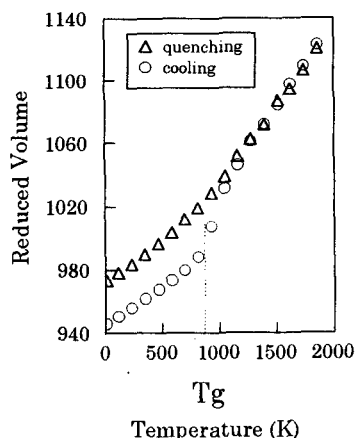


Fig. 2. Temperature dependence of the volume in cooling and quenching procedures.

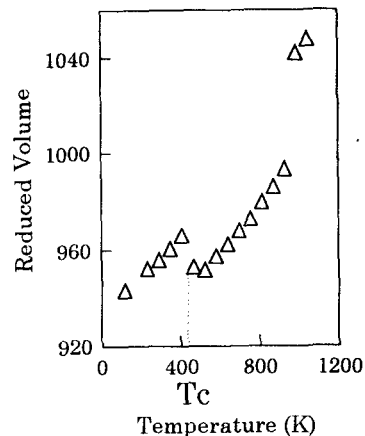


Fig. 3. Temperature dependence of the volume of amorphous alloy at a crystallization process.

(10^{11} – 10^{16} K/sec) by executing the stepwise temperature reduction. Then it was heated up at a slow rate ($\sim 10^{12}$ K/sec) until it melted down completely.

4. RESULTS

We can see the phases of the simulation system by monitoring macroscopic observables such as the averages of enthalpy, internal energy and volume of the system, as well as microscopic ones as the radial distribution between particles, time evolution of mean square displacements of atoms and, of course, atomic configuration itself. Particularly, under the constant pressure condition, the temperature dependence of the volume of the system helps us to know the phases of the system.

Typical temperature dependence of the volume of the system are shown in Fig. 1, Fig. 2 and Fig. 3. The reduced volume is expressed in a unit of 3.94 \AA^3 . The dependence of the volume of Ti-38at.%Al alloy system on the temperature during a slow-cooling and heating cycle is plotted in Fig. 1, in which open circles and open triangles correspond to the cooling and the heating processes, respectively. Because of the high order of changing rates in temperature, a considerable hysteresis is observed. Supposed that the hysteresis is caused by the existence of a supercooled state, we can estimate the melting point T_m of the alloy system as depicted in the figure. In Fig. 2 the volume-temperature relation of the same system in a rapid-cooling (quenching) procedure is plotted by open triangles, together with that in a slow-cooling procedure plotted by open circles. In the quenching process the volume changes linearly in separate two regions. The high-temperature region with higher slope corre-

sponds to liquid states and the low-temperature region with lower slope corresponds to amorphous states. This discontinuity in slope indicates a liquid-amorphous transition and thus we can identify the glass transition temperature T_g as shown in the figure. A typical temperature dependence of the volume in a heating procedure from an amorphous state is also shown in Fig. 3 in the case of Ti-94at.%Al alloy system. A jump of the trajectory at about $T = 400$ K corresponds to amorphous-crystal transition, by which we define the crystallization temperature T_c of the amorphous.

Thus we have the concentration dependence of the melting point T_m , the glass transition temperature T_g and the crystallization temperature T_c of amorphous alloys in the system, which are shown in Fig. 4 by open circles, open squares and open triangles, respectively, with interpolating curves. For T_m , we obtained consistent results with the experimental measurements, while we found two times higher values in the

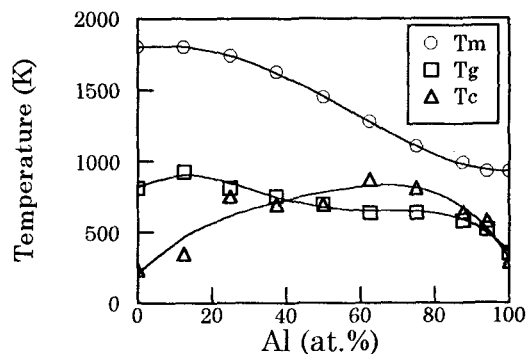


Fig. 4. T_m , T_g and T_c plotted as a function of the concentration of Al.

simulations using Lennard-Jones potentials. For T_g , although there are no experimental measurements to compare, high value of T_g/T_m ratio in Al-rich concentration range found in Fig. 4 means that the amorphous would be likely to form in the same Al-rich region. We must note that the cooling rate dependence of T_g reported in other simulations¹⁰ could not be detected in our simulations. As for T_c , although plotted data include the wide error bars, they are consistent with the experimental observations².

Fig. 5 shows the phases of the endpoint of the system after cooling run in the cooling rate - Al concentration plane. Open circles denote amorphous states, while open triangles denote crystalline states. We can see that the critical value of cooling rate for amorphization has wide distribution in magnitude of order 10^3 , and has asymmetrical dependence on Al concentration with its minimum in Al-rich region. For comparison, the results of analogous simulations using Lennard-Jones potentials are plotted by closed symbols, which indicate higher critical cooling rates and less concentration dependence.

For observed crystalline states, the system always formed a close-packed structure, that is, fcc structure or hcp structure with or without stacking faults. Although our EAM potentials are set to fulfill the conditions that the minimum energy state takes fcc structure in Al-rich concentration region and that it takes hcp structure in Ti-rich region, the crystalline structures obtained in the simulations seemed not to follow such concentration dependence. Moreover, some crystals occasionally contained one or two vacancies. All these are because the cooling rates were actually so high that the system could not afford to settle down to its minimal energy state and that it

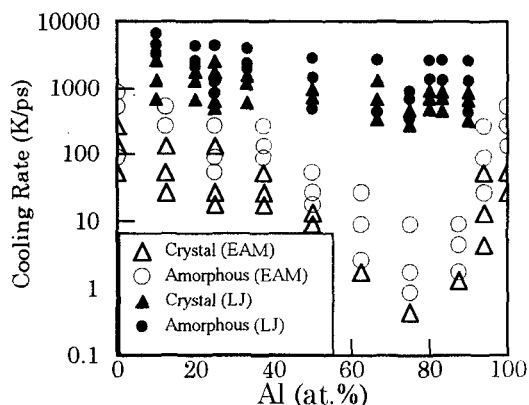


Fig. 5. Structure map of the Ti-Al system after cooling procedure.

should easily be trapped at a metastable state. By the same reason, we could not observe an atomic ordering with long range correlation such as $L1_0$ structure. In addition, no intermediate states could not be observed in the crystallization processes of the amorphous alloys. That is mainly because such metastable states are too fragile to appear in a detectable period under high heating rates of the simulations.

5. DISCUSSION

We have obtained the results reproducing the thermodynamic properties of Ti-Al system together with the experimentally observed concentration range (40~85 at.% Al) for amorphization but failed in demonstrating the emergence of intermediate states during amorphous-crystal transition processes. Now we further proceed to the study of the mechanism of amorphization in Ti-Al system by investigating the structural properties of the amorphous alloys obtained in the simulations. From observations^{9,10} in both experiments and computer-simulations, it is well known that icosahedral structures are the basic building blocks of amorphous state in monatomic systems. The fact that the discrepancy between the atomic radius of Ti and that of Al is rather small (a few percent) prompted us to search such icosahedral structures in the simulated Ti-Al amorphous alloys.

As depicted in Fig. 6, we observed a number of icosahedral clusters in the amorphous states obtained in the simulations. In Fig.6(a), light-gray spheres denote Al atoms and dark-gray ones denote Ti atoms, and color of each icosahedron in Fig.6(b) corresponds to that of the atom at the central position of the cluster. As seen from the figures, most of icosahedral clusters have Al atom in their center. The abundance of Al-centered clusters is observed in amorphous alloys irrespective of Ti-Al atomic ratio of the system.

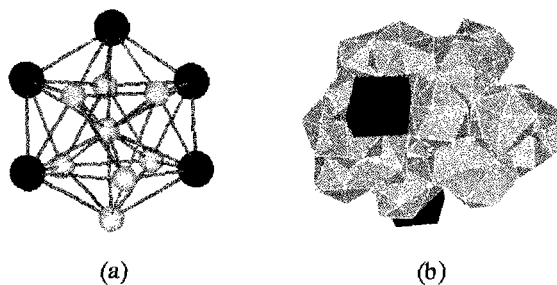


Fig. 6. Icosahedron (a) and a network of icosahedral clusters (b) found in a Ti-75at.%Al amorphous alloy.

Then, from an energetical point of view, we have first evaluated the lowest energy of the icosahedral cluster with a definite atomic composition among the possible configurations in both Al-centered and Ti-centered cases. The results are shown in Fig. 7. We can see that the Al-centered cluster has lower energy for any composition. Next, as an estimation of the cluster stability against crystallization, we have evaluated the energy difference between icosahedral cluster and its fcc crystal counterpart, which can be constructed from the icosahedral cluster by small atomic displacements, as illustrated in Fig. 8. The results plotted in Fig. 8 indicate that Al-centered icosahedral clusters should be more stable. In addition, analogous estimation based on Lennard-Jones potentials showed less energetic dependence of the configuration of the clusters.

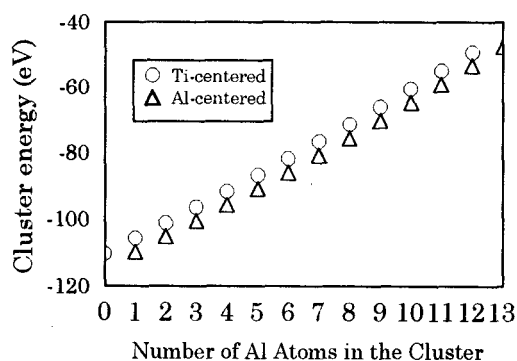


Fig. 7. Variation of energy of icosahedron with the number of Al atoms in the cluster.

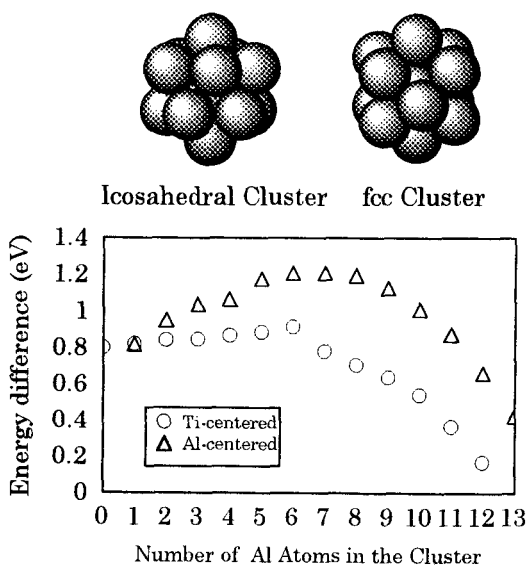


Fig. 8. Variation of energy difference between icosahedral cluster and fcc cluster with the number of Al atoms in the cluster.

Above results suggest that the stability of the icosahedral clusters is increased by the nature of EAM potentials. In other words, the higher stability of Al-centered icosahedral clusters is not only brought from the fact that the atomic radius of Al is a little smaller than that of Ti, which is essentially two-body effect, but also from the fact that the electron density of Al atom is higher than that of Ti, which induces the asymmetry of many-body effect in EAM scheme. Thus we can conclude that the basic building blocks for amorphous states of the Ti-Al system should be Al-atom centered icosahedral clusters, which are stabilized by many-body effect.

Finally we shall comment on finite size effects in the simulation. The order of the critical cooling rates obtained in the simulations is higher than those accessible by the sputtering experiments ($\sim 10^{12}$ K/sec in maximum¹¹). However, the results by using larger simulation systems indicate¹² that the critical cooling rate for amorphization could be reduced to the amount of about one order, by which the discrepancy above mentioned would be dissolved.

REFERENCES

1. H. Onodera, T. Abe and T. Tsujimoto, *Current Advances in Materials and Processes* 6 (1993) 627.
2. T. Abe, S. Akiyama and H. Onodera, *ISIJ International* 34 (1994) 429.
3. M. S. Daw and M. I. Baskes, *Phys. Rev. Lett.* 50 (1983) 1285; *Phys. Rev.* B29 (1984) 6443.
4. D. J. Oh and R. A. Johnson, *J. Mater. Res.* 3(1988)471.
5. R. A. Johnson, *Phys. Rev.* B39 (1989) 12554.
6. R. Hultgren et al., *Selected Values of the Thermodynamic Properties of Binary Alloys* (American Society for Metals, Metals Park, OH, 1973).
7. J. M. Sanchez, J. R. Barefoot, R. N. Jarrett and J. K. Tien, *Acta metall.* 28 (1980) 651.
8. M. Parrinello and A. Rahman, *Phys. Rev. Lett.* 45 (1980) 1196.
9. J. Farges, M. F. de Feraudy, B. Raoult and G. Torchet, *J. Chem. Phys.* 78 (1983) 5067; 84 (1986) 3491.
10. F. Yonezawa, "Glass Transition and Relaxation of Disordered Structures", in *Solid State Physics* (1991) Vol. 45, and references therein.
11. K. Sumiyama, *Bulletin of the Japan Institute of Metals* 25 (1986) 615.
12. M. Shimono and H. Onodera, "Molecular Dynamics Study on Amorphization of Ti-Al Alloys", in *CMSMD* 96 (1996) ed. S. Nishijima and H. Onodera.